Journal of Alloys and Compounds 509 (2011) 1866–1869

Contents lists available at ScienceDirect

Journal of Alloys and Compounds

journal homepage: www.elsevier.com/locate/jallcom

The correlation between as-cast and aged microstructures of high-vacuum die-cast Mg–9Al–1Zn magnesium alloy

Jie Song, Shou-Mei Xiong*

State Key Laboratory of Automotive Safety and Energy, Department of Mechanical Engineering, Tsinghua University, Tsinghua Garden, Haidian District, Beijing 100084, China

ARTICLE INFO

Article history:
Received 4 July 2010
Received in revised form 17 October 2010
Accepted 22 October 2010
Available online 30 October 2010

Keywords:
Alloys
Aging
Microstructure
Precipitation

ABSTRACT

The aging microstructure of high-vacuum die-cast Mg–9Al–1Zn magnesium alloy was investigated. The microstructure after aging at the surface of the cast specimens was different than the center, which could be attributed to the differences in as-cast microstructure and Al content in these two regions. Both regions showed discontinuous precipitation characteristics; these precipitations started from the β-particles, which initially precipitated at the grain boundaries and then grew to the inner grains. The Al content greatly influenced the growth rate and overall percentage of the discontinuous precipitated structures.

1. Introduction

Magnesium and its alloys are the lightest metallic structural materials with superior mechanical properties, and their attractiveness for a variety of industrial applications in the automobile, aeronautic and aerospace industries is well known [1,2]. The Mg–9Al–1Zn (AZ91D) magnesium alloy is one of the most popular die-casting magnesium alloys due to its superior mechanical properties (strength and ductility) and castability [3]. Previous heat treatment studies on the alloy have shown that the precipitation mode of aging induces both discontinuous precipitation (DP) and continuous precipitation [4–9]. Bradai et al. [10,11] found a new mode of the discontinuous dissolution reaction in magnesium alloy during a special cyclic heat treatment, and they presented the relationship between the grain boundary (GB) and the DPs. The kinetics of the aging procedure was also studied by Duly and Cerri [12,13]. However, there have been few examinations of the aging treatment of high-vacuum die-cast (HVDC) magnesium alloys. In this paper, HVDC specimens of AZ91D alloy were used to investigate the microstructure changes after aging.

2. Experimental method

The HVDC specimens of AZ91D (Mg–8.91 wt.%Al–0.73 wt.%Zn–0.22 wt.%Mn) alloy were sectioned from shock tower castings with dimensions of 100 mm × 30 mm × 3 mm (length, width and height). The vacuum level of the casting process was approximately 5 KPa to decrease the porosities in the final cast parts. The specimens were divided into three groups: as-cast, solution treated (T4 treatment, solution treated at 686 K for 16 h, then quenched at 338 K in hot water), and aged (aged at 441 K for 2, 4, 8 and 16 h separately after T4 treatment), according to the ASTM B61-03 standard. The specimens were buried in magnesia powders to avoid oxidation of the specimens during the heat treatment processes. The specimens for XRD, SEM and TEM examinations were cut from the center of the specimens. XRD analysis was conducted on specimens grounded with SiC abrasive papers of up to 2000 grit, using a D/max-2550 X-ray automatic powder diffractometer, operated at 200 mA and 45 kV, using Cu Ka radiation. The XRD scans were acquired from 20° to 90° with a step size of 0.02° and a dwell time of 6°/min. The specimens for microstructure observation were examined using SEM with EDS. After the XRD analysis, the specimens were then polished with oil-based diamond compounds 1 μm in size and subsequently etched at room temperature using a nitric glycol etching agent (1 ml nitric acid, 75 ml ethylene glycol, and 24 ml distilled water) to reveal the β-phase distribution and to detect the macro-segregation at the surface and the center of the specimens. ICP (inductively coupled plasma) was used to analyze and achieve average Al element content on large scale (skin and center regions). The specimens for ICP testing were picked out by milling. These specimens included skin and center regions in as-cast, solution and aging statues. The preparation procedure for the TEM specimens contained the following steps: first, slices of 0.2 mm thickness were cut from the center of the specimens. Next, the slices were mechanically polished and cut into disks with a diameter of 3 mm, and dimpled to about 20 μm in the center. Finally, the specimens underwent ion milling using a Gatan precision ion polishing system 691 under conditions of 5.0 kV and incident angle of 8°. All the TEM specimens were examined by a JEOL 2010 TEM.

3. Results and discussion

3.1. The microstructure of the as-cast, solution treated and aged states

The microstructure of the as-cast, solution treated and aged specimens were analyzed by the XRD (Fig. 1). It was found that

* Corresponding author. Tel.: +86 10 62773793; fax: +86 10 62770190.
E-mail address: smxiong@tsinghua.edu.cn (S.-M. Xiong).

0925-8388/$ – see front matter © 2010 Published by Elsevier B.V.
doi:10.1016/j.jallcom.2010.10.075

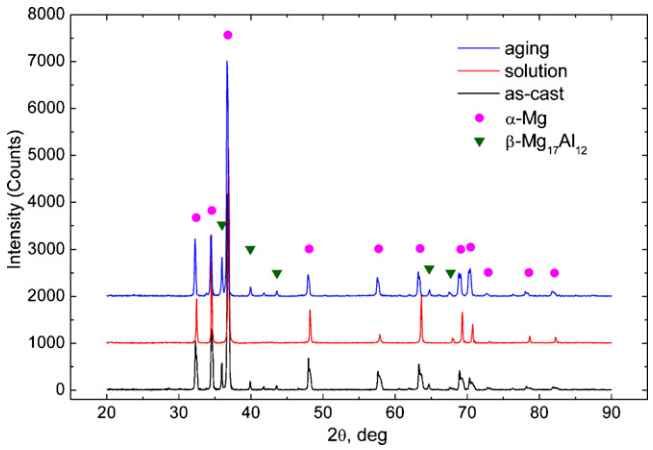

Fig. 1. XRD results of the as-cast, solution treated and aged specimens.

most of the β-$Mg_{17}Al_{12}$ phase dissolved in the α-matrix during the solution treatment and then reemerged during the aging process. The microstructure characteristics of the specimens of as-cast and T6 (aging for 16 h after T4 treatment) status are shown in Fig. 2. Fig. 2a and b shows that the microstructures exhibited obvious differences between the surface and the center regions, respectively, which were separated by the segregation bands [14] that can be seen clearly in Fig. 5f. The coarse α-dendrite was observed in the center region (Fig. 2a). However, a fully divorced eutectic (DE) pattern was observed in the surface region, where the β-phases are more homogenous than in the center region (Fig. 2b). Fig. 2c and d shows the microstructure of the specimens containing the DP areas and α-matrix after T6 treatment. It is evident that the surface region contains more DP areas than the center region. In addition, the DPs generally grew from the original location at the grain boundary and the typical characteristics can be observed in Fig. 2c. Fig. 2e shows a magnified image of the microstructure of the T6 specimens of the DPs in the circled area in Fig. 2d and the magnified image of the inhomogeneous microstructure of the α-matrix in the rectangular area of Fig. 2d is shown in Fig. 2f. The white spots in Fig. 2e are the β-phases which were unable to dissolve completely during the

Table 1
The Al content in different areas (wt.%).

	Surface	Center	Cross section
As-cast	9.5	8.3	8.9
Solution-4 h	9.6	8.4	9.1
Solution-32 h	9.6	8.3	8.8

T4 treatment. According to the ICP analysis shown in Table 1, the average composition of Al at the center and surface areas is different, and it was also found that the concentration of Al was not significantly affected by the heat treatment process.

The microstructure and Al content differences in the surface and center regions could be explained by the "Swqueira theory", which states that the dendrites forming in die castings must be formed in the shot sleeve [15]. Because of the different solidification and filling conditions between the surface and the center regions, the difference in Al concentration in the two regions was caused by bands of segregation and bands of porosities [14]. These bands of segregation or porosities have been well analyzed by Dahle's group [14]. These bands can also act as barrier of preventing Al element diffusion in the followed solution treatment process. The lower Al concentration in the coarse dendrites (5 wt.% Al) could decrease the Al content in the center area, resulting in a higher Al concentration in the remaining Mg melt. Due to the rapid solidification of the remaining Mg melt against the die wall, a homogenous microstructure (i.e. the uniform β-phase distribution) with a higher Al content was formed. The β-phase dissolved and diffusion of Al could proceed in the subsequent solution treatment, leading to only α-matrix after solution treatment. In the current study, a 15 min solution treatment led to a uniform α-matrix, and the Al content became homogenous in each region (the surface and the center) with longer solution treatment. Because of the existence of the segregation band, the Al element could hardly diffuse between the two regions and the difference in Al concentration between the regions will remain the same after the T4 treatment as in the as-cast state.

3.2. The precipitation mode

During the aging process, more time is needed for the diffusion of the Al element to precipitate the β-phase at a lower aging tem-

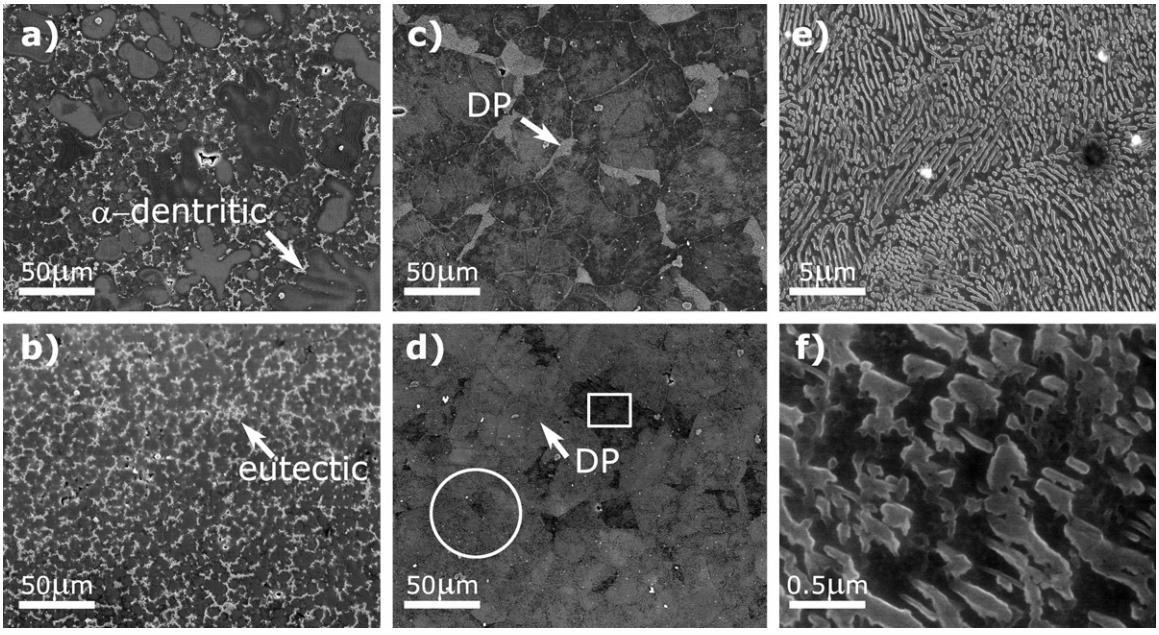

Fig. 2. SEM images of microstructure features: center (a) and surface (b) regions of as-cast status of high vacuum die-cast specimens; center (c) and surface (d) regions after T6 heat treatment; at a higher magnification of round shape (e) and rectangle shape (f) regions from Fig. 2d.

perature. In this research, the un-dissolved β-phase during the T4 process did not affect the subsequent aging mode or the DP initiation location (i.e. these particles could not act as the nuclei or substrates of the DPs). These coarse β-particles were unsuitable to act as nuclei because their size was usually larger than the width of the lamellar precipitated β-lath. In fact, the nuclei of the DPs were formed along the GBs at the early stage of aging. This is because of the difference in diffusibility between GBs and the inner grains and the much lower diffusion resistance force along the GBs [16], as well as the higher Al concentration at the grain boundary due to insufficient diffusion. The precipitated lamellate grew on the pre-precipitated β-particles on the GBs to the inner grains, which was diffusion controlled [17]. Fig. 3 clearly shows the β-phase particles first emerging at the initial GBs before the formation of DPs. The DPs then grew from these precipitated particles, which have a parabolic morphology. This process was observed as the supersaturated α-Mg solution precipitated a new phase (β-$Mg_{17}Al_{12}$) with (α + β) as the equilibrium state. The lath parabolic morphology (DPs) consists of alternative layers of α and β phases.

In addition, the lath shape DPs and the α-matrix show a habit relationship. Fig. 4 shows a typical TEM microstructure of the specimens after T6 heat treatment with the DP area and the α-matrix. The selected area diffraction (SAD) patterns taken from the interface of the DP and the matrix showed that the α-matrix and the β precipitation have a habit relationship with $\{1\,0\,-1\,1\}_\alpha||\{1\,1\,0\}_\beta$ and $\langle -1\,2\,-1\,0\rangle_\alpha||\langle 1\,-1\,1\rangle_\beta$. This could be explained by the similar lattice structure of the two phases and by the fact that the lattice distance of the β-$Mg_{17}Al_{12}$ plane $\{1\,1\,0\}_\beta$ is about three times wider than the α-matrix plane $\{1\,0\,-1\,1\}_\alpha$.

3.3. *The influences of Al content and as-cast microstructure on the precipitation process*

The evolution of the DPs at different aging times is shown in Fig. 5. It can be observed that the DP regions appeared and grew in both the surface and the center regions along the GBs with increasing aging time. The growth rate of the DPs was faster in the surface region than in the center, evidenced by the larger amount of DP areas in the surface region after the same aging time. The DPs for-

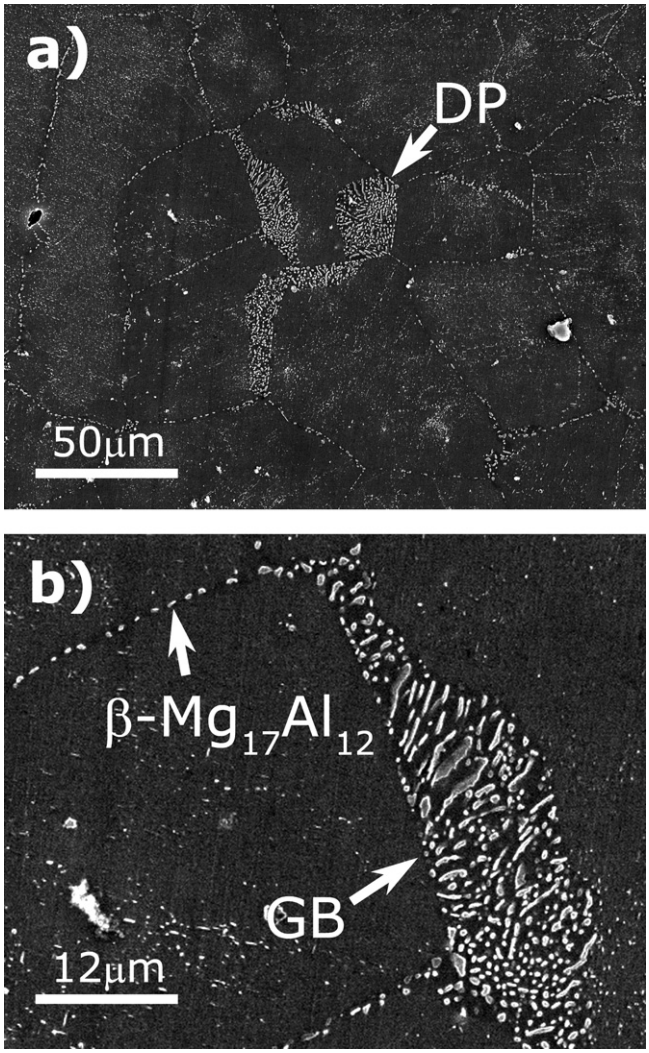

Fig. 3. (a) Morphology of the discontinuous precipitation along the grain boundary; (b) distribution of the β-phase along the grain boundary.

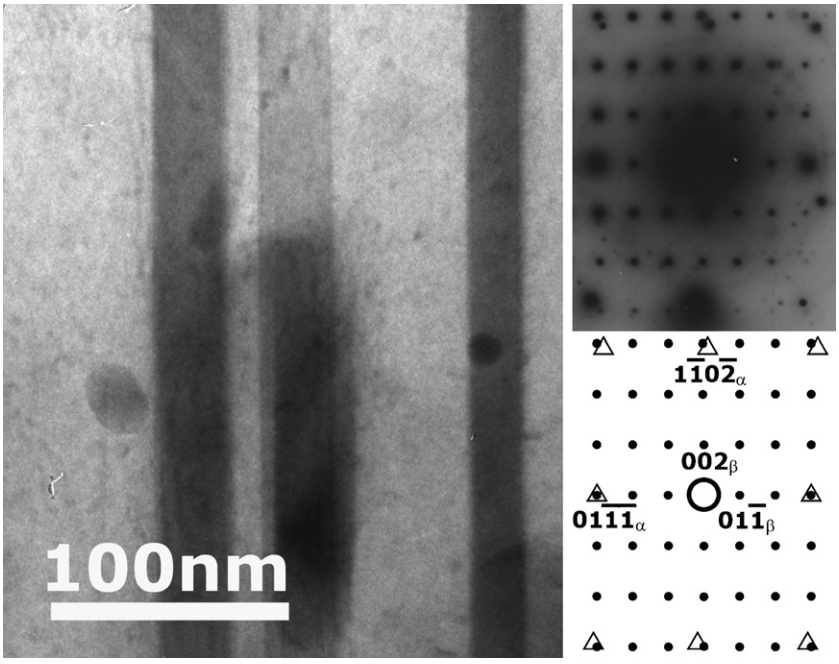

Fig. 4. TEM images of the discontinuous precipitation of the aging specimen (the SAD pattern was taken from the interface of the discontinuous precipitation and matrix).

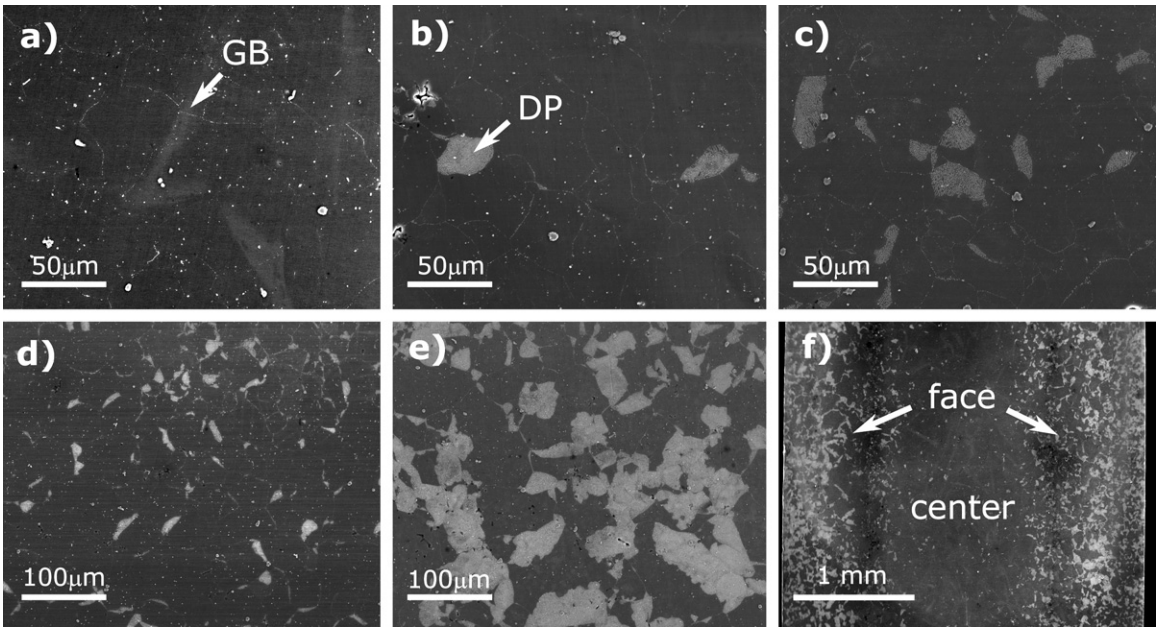

Fig. 5. The discontinuous precipitations' evolution at the center region with the aging time of 2 h (a), 4 h (b) and 8 h (c); at the surface region with the aging time of 2 h (d) and 4 h (e); (f) cross section of the specimen with the aging time of 4 h.

mation and growth on the GBs in the surface area could be clearly observed after 2 h aging time (Fig. 5d), while there were no DPs in the center area after the same period of aging time (Fig. 5a). After 4 h aging time, approximately 80% of the microstructure in the surface region was changed to DPs (Fig. 5e), while there were much fewer DPs in the center region (Fig. 5b) even after 8 h aging time (Fig. 5c). The difference in the amount of the DPs after the same period of aging time may have been caused by the as-cast microstructure differences. As mentioned before, the surface region has a more uniform microstructure and higher Al content. In contrast, the as-cast microstructure of the center region has a DE microstructure and coarse dendrites with lower Al concentration (compared with the skin region, the quantity of DE in the center region was much lower). This means that the Al element would be higher in the DE region, which is always located among the coarse dendrites (usually the GBs), and thus this area is more liable to precipitate the β-phase during the aging process. The percentage of DPs in the surface region increased with aging time. After 4 h of aging time, most of this area was covered with DPs. Therefore, the growth velocity between the two regions was mainly influenced by the Al content. A higher Al element in the T4 microstructure would facilitate the diffusion controlled β-phase formation and growth process.

4. Conclusions

The effects of different aging time on the precipitation behavior of the HVDC AZ91D alloy specimens in the surface and center regions were studied using microscopy analysis. Both the surface and center regions of the HVDC specimens of AZ91D alloy had the same precipitation mode during aging and the precipitation mode was DP. The β-phase particles first precipitated at the grain boundaries, and these particles acted as nuclei from which the growth of the DPs started. During the aging treatment, the surface region formed the DPs to a greater extent than the center region. This could be attributed to the higher Al concentration in the surface region, which reduced the diffusing time of the Al element and the formation time of the β-phase during aging, thereby greatly accelerating the growth velocity of the β-phase lath and the formation of the DPs.

Acknowledgements

This research was financially supported by the National High Technology Research and Development Program of China (2009AA03Z114). The authors would like to thank Dr. Kumar Sadayappan from CANMET Materials Technology Laboratory, Canada, for providing all the test coupons for the current research.

References

[1] R.M. Wang, A. Eliezer, E.M. Gutman, Mater. Sci. Eng. A 355 (2003) 201.
[2] J.P. Weiler, J.T. Wood, R.J. Klassen, R. Berkmortel, G. Wang, Mater. Sci. Eng. A 419 (2006) 297.
[3] M.X. Zhang, P.M. Kelly, Scripta Mater. 48 (2003) 647.
[4] A.F. Crawley, K.S. Milliken, Acta Metall. 22 (1974) 557.
[5] D. Duly, Y. Brechet, Acta Metall. Mater. 42 (1994) 3035.
[6] D. Duly, M.C. Cheynet, Y. Brechet, Acta Metall. Mater. 42 (1994) 3843.
[7] D. Duly, M.C. Cheynet, Y. Brechet, Acta Metall. Mater. 42 (1994) 3855.
[8] D. Duly, J.P. Simon, Y. Brechet, Acta Metall. Mater. 43 (1995) 101.
[9] S. Celotto, Acta Mater. 48 (2000) 1775.
[10] D. Bradai, P. Zieba, E. Bischoff, W. Gust, Mater. Chem. Phys. 72 (2001) 401.
[11] D. Bradai, P. Zieba, E. Bischoff, W. Gust, Mater. Chem. Phys. 78 (2003) 222.
[12] D. Duly, Y. Brechet, B. Chenal, Acta Metall. Mater. 40 (1992) 2289.
[13] E. Cerri, S. Barbagallo, Mater. Lett. 56 (2002) 716.
[14] A.K. Dahle, D.H. StJohn, Acta Mater. 47 (1998) 31.
[15] W.P. Sequeira, M.T. Murray, G.L. Dunlop, D.H. St. John, TMS Annual Meeting, 1997, p. 169.
[16] Y. Mishin, C. Herzig, Mater. Sci. Eng. A 260 (1999) 55.
[17] J.W. Christian, The Theory of Transformations in Metals and Alloys, Pergamon, Oxford, 2002, p. 508.